

---

# NoteLLM-2: Multimodal Large Representation Models for Recommendation

---

Chao Zhang<sup>1,2</sup>, Haoxin Zhang<sup>3</sup>, Shiwei Wu<sup>1,2</sup>, Di Wu<sup>3</sup>,  
Tong Xu<sup>1,2\*</sup>, Yan Gao<sup>3</sup>, Yao Hu<sup>3</sup>, Enhong Chen<sup>1,2\*</sup>

<sup>1</sup>University of Science and Technology of China

<sup>2</sup>State Key Laboratory of Cognitive Intelligence

<sup>3</sup>Xiaohongshu Inc.

{zclfe00,dwustc}@mail.ustc.edu.cn, {tongxu,cheneh}@ustc.edu.cn,  
{zhanghaoxin,yadun,xiahou}@xiaohongshu.com, wudi1123@foxmail.com

## Abstract

Large Language Models (LLMs) have demonstrated exceptional text understanding. Existing works explore their application in text embedding tasks. However, there are few works utilizing LLMs to assist multimodal representation tasks. In this work, we investigate the potential of LLMs to enhance multimodal representation in multimodal item-to-item (I2I) recommendations. One feasible method is the transfer of Multimodal Large Language Models (MLLMs) for representation tasks. However, pre-training MLLMs usually requires collecting high-quality, web-scale multimodal data, resulting in complex training procedures and high costs. This leads the community to rely heavily on open-source MLLMs, hindering customized training for representation scenarios. Therefore, we aim to design an end-to-end training method that customizes the integration of any existing LLMs and vision encoders to construct efficient multimodal representation models. Preliminary experiments show that fine-tuned LLMs in this end-to-end method tend to overlook image content. To overcome this challenge, we propose a novel training framework, NoteLLM-2, specifically designed for multimodal representation. We propose two ways to enhance the focus on visual information. The first method is based on the prompt viewpoint, which separates multimodal content into visual content and textual content. NoteLLM-2 adopts the multimodal In-Content Learning method to teach LLMs to focus on both modalities and aggregate key information. The second method is from the model architecture, utilizing a late fusion mechanism to directly fuse visual information into textual information. Extensive experiments have been conducted to validate the effectiveness of our method.

## 1 Introduction

With the development of the internet, most online platforms are full of multimodal information to drive user engagement [51, 50, 53]. Multimodal recommendation is a necessary service for these platforms [30], which recommends items based on users' interest on item multimodal information. These techniques mainly rely on multimodal representations, extracting raw multimodal content into dense embeddings [61], and then measuring similarity through these multimodal embeddings. The enhancement of multimodal representations can fundamentally improve numerous downstream tasks, such as retrieval [31], clustering [34], and item modeling [60, 51].

Many existing works have investigated multimodal representations, such as CLIP [37], METER [14] and Siglip [58]. Although great success has been achieved in these domains, the number of parameters

---

\*Corresponding Authors

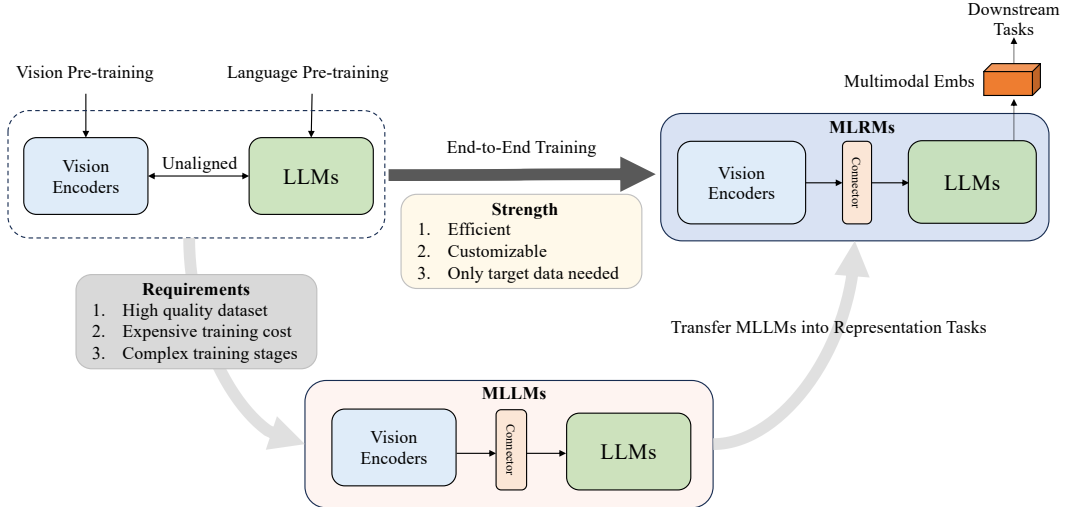


Figure 1: Two strategies for using LLMs to enhance multimodal representations.

in most multimodal representation models still possesses the large potential for scaling [45, 46]. However, existing works [45, 46] primarily focus on scaling vision models to improve multimodal representation, overlooking the textual branch. At the same time, due to the lack of sufficient pure text-oriented pre-training [37, 45, 46, 58], the text branch in multimodal representation models often exhibits suboptimal understanding of text information [6, 59]. Therefore, it is necessary to enhance text understanding in multimodal representations models.

Recently, Large Language Models (LLMs) have shown impressive capabilities in text understanding and generating [18, 7, 2, 47]. Several works show the superior performance of LLMs in generating textual embeddings [34, 60, 19, 31, 4]. However, the use of LLMs for enhancing text understanding in multimodal representations is underexplored. As shown in Figure 1, one feasible method is to adapt Multimodal Large Language Models (MLLMs) [29, 25, 2, 22] for representation tasks. Nevertheless, pre-training MLLMs requires collecting high-quality, web-scale multimodal data, resulting in complex training procedures and high costs [25, 2]. This leads the community to rely heavily on open-source MLLMs, hindering customized training using the most advanced LLMs and vision encoders for representation scenarios. Therefore, we aim to design an end-to-end training method that customizes the integration of any existing LLMs and vision encoders to construct efficient multimodal representation models. This end-to-end method is practical when the target LLMs lack pre-trained visual components [11, 18, 1], as it only needs target domain data, eliminating pre-training data collection. Besides, we can optimize the customized model structure for representation tasks to achieve better efficiency while ensuring performance. We call these models for enhancing multimodal representation with LLMs as Multimodal Large Representation Models (MLRMs).

In this work, we explore MLRMs in item-to-item (I2I) multimodal recommendation scenarios. We conduct fine-tuned preliminary experiments to examine our goal. Our findings reveal that representations of naive fine-tuned end-to-end MLRMs are biased towards textual information, ignoring visual content. Visual information is mainly used to amplify the key element in multimodal content, rather than being directly aggregated by representations. To solve this challenge, we propose a novel training framework, called NoteLLM-2, for multimodal representation tasks. We design two methods to mitigate visual modality neglect. The first method is multimodal In-Context Learning (mICL). This method separates multimodal content into visual and textual components, subsequently compressing the content into two modality-compressed words. Each modality-compressed word conducts in-batch contrastive learning with its corresponding modality-compressed word. During inference, mICL can aggregate multimodal information in an In-Context Learning (ICL) way [12, 48]. The second method is the late fusion mechanism. Most MLLMs adopt early fusion, which maps visual features into the textual feature space of LLMs and interact visual features with text embeddings through LLMs [29, 25, 2, 22]. Even though early fusion can deepen the multimodal information interaction, it can easily lead to the loss of pure visual information during the multimodal fusion conducted by LLMs [25, 62]. We incorporate late fusion based on early fusion, retaining more

visual information by delaying the fusion process. Specifically, we adopt a multimodal gate fusion mechanism [8], which takes visual representations from the visual encoder and representations from the LLM to generate final multimodal representations. We conduct extensive experiments to demonstrate our NoteLLM-2 effectiveness. Our paper makes the following contributions:

- To the best of our knowledge, we are the first to explore the multimodal representation assisted by LLMs. We propose an end-to-end training method that customizes the integration of any existing LLMs and vision encoders to form efficient MLRMs.
- We reveal that fine-tuning unaligned MLRMs for representation tasks can cause the modality imbalance, overlooking visual information. To overcome this problem, we design a novel framework, NoteLLM-2, which contains two mechanisms, mICL and late fusion.
- Extensive experiments have demonstrated the effectiveness of our proposed framework for multimodal recommendation representation.

Our paper is organized as follows: We begin with a preliminary investigation of MLRMs in multimodal I2I recommendation scenarios and analyze the results. Then, inspired by this analysis, we design our NoteLLM-2. And we conduct experiments to demonstrate the effectiveness of our NoteLLM-2. Besides, related works and additional details are presented in Appendix A.

## 2 Preliminary Investigation

### 2.1 Preliminaries

**Problem Statement.** In our scenarios, every item represents a note, which is generated by users and expresses their life experiences. We show some notes in Appendix H. We assume  $\mathcal{N} = \{n_1, n_2, \dots, n_m\}$  as note pool, where  $m$  is the number of notes. Each note contains textual information, like the title, topic, and content, as well as the image. We denote the  $i$ -th note as  $n_i = (t_i, tp_i, ct_i, v_i)$ , where  $t_i, tp_i, ct_i, v_i$  mean the title, the topic, the content and the image respectively. Given a query note  $n_i$ , the I2I recommendation system ranks the note pool  $\mathcal{N} \setminus \{n_i\}$  according to the multimodal content similarity to the given note. The objective of this system is to prioritize the ranking of the related target note.

**Dataset Construction.** Following [60], we utilize the co-occurrence mechanism to build related note pairs based on user behaviors without human annotations. This mechanism assumes that notes frequently read together are likely related. Then, we count the co-occurrence score in which users viewed note  $n_A$  and subsequently clicked on note  $n_B$  as follows:

$$s_{n_A \rightarrow n_B} = \sum_{u \in U_{n_A \rightarrow n_B}} \frac{1}{N_u}, \quad (1)$$

where  $s_{n_A \rightarrow n_B}$  means the co-occurrence score from note  $n_A$  to note  $n_B$ ,  $U_{n_A \rightarrow n_B}$  is the set of users who viewed note  $n_A$  and subsequently clicked on note  $n_B$ , and  $N_u$  denotes the quantity of the note set clicked by the user  $u$  in the user behavior data. After calculating the co-occurrence score for all note pairs, we construct the set of co-occurrence scores  $\mathcal{S}_{n_i}$  from note  $n_i$  to all other notes. Specifically,  $\mathcal{S}_{n_i}$  is defined as  $\{s_{n_i \rightarrow n_j} | 1 \leq j \leq m, i \neq j\}$ . Next, we remove outlier from  $\mathcal{S}_{n_i}$  with co-occurrence scores above *up* or below *low*. Finally, we select the  $t$  notes with the highest co-occurrence scores from the filtered set as the related notes for note  $n_i$ .

**Basic Representation Method of MLRMs.** Following [19], we adopt a prompt with explicit one word limitation to compress the multimodal content into one embedding. Specifically, we use json format to show note content and our prompt is the following:

**Note Compression Prompt**

Note content: {'image': <IMG>, 'title':  $t_i$ , 'topic':  $tp_i$ , 'content':  $ct_i$ }. Compress this note into one word."

In this template, <IMG> is a placeholder, which will be replaced by vision embeddings processed from raw images  $v_i$ .

The overall framework is shown in Figure 2 (a). This framework first utilizes the vision encoder  $V_\theta$  to extract the pre-processed image  $v_i$  into visual features  $Z_v \in \mathbb{R}^{L \times h_v}$  in the notes  $n_i$ , where  $L$

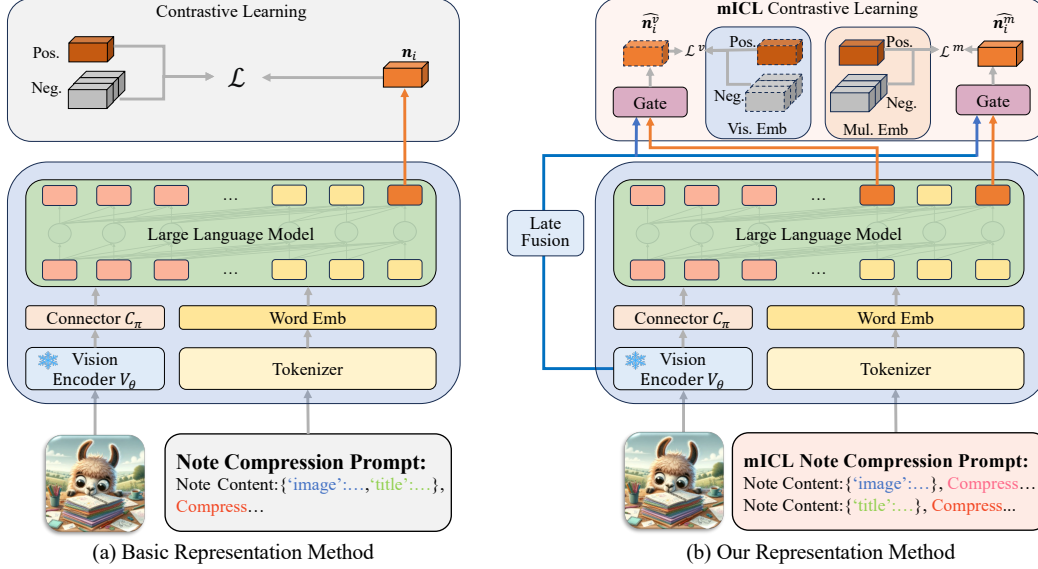


Figure 2: The frameworks of MLRMs. (a) is the basic method for representations. (b) is our representation method, which contains two easy and effective mechanisms to enhance multimodal representation ability, mICL and late fusion.

is the length of visual features,  $h_v$  is the dimension of visual features and  $Z_v = V_\theta(v_i)$ . Then, the connector  $C_\pi$  transforms the visual features  $Z_v$  into the word embedding space of LLMs to form visual embeddings  $E_v \in \mathbb{R}^{L_c \times h_t}$ , where  $L_c$  is the length of visual embeddings input into LLMs,  $h_t$  is the dimension of LLMs' hidden states and  $E_v = C_\pi(Z_v)$ . After processing images, the text prompts are tokenized into discrete indexes, then form the text word embedding  $E_t \in \mathbb{R}^{T \times h_t}$ , where  $T$  is the length of text tokens. To insert the visual embeddings into the correct position in text embeddings, we replace word embeddings in positions of the  $\langle \text{IMG} \rangle$  token by the visual embeddings  $E_v$ , forming the multimodal embeddings  $E_m \in \mathbb{R}^{(L_c+T-1) \times h_t}$ . Last, we use LLMs  $LLM_\mu$  to process the multimodal embeddings to generate last hidden states  $H \in \mathbb{R}^{(L_c+T-1) \times h_t}$ , where  $H = LLM_\mu(E_m)$ . We take last embeddings of  $H$  as the note representation  $n_i$  for note  $n_i$ . This method constrains LLMs to compress the multimodal content into one embedding in the form of the next token prediction.

However, LLMs are trained using the language modeling loss [29, 25, 3, 22], which significantly differs from representation tasks. To bridge this gap, we employ contrastive learning, a prevalent technique for training embeddings [34, 60, 19, 31]. Specifically, each minibatch contains  $B$  related note pairs  $(n_i, n_i^+)$ , resulting in a total of  $2B$  notes per minibatch. Following [36], we use gradient descent to minimize the contrastive loss as follows:

$$\mathcal{L}(\pi, \mu) = -\frac{1}{2B} \sum_{i=1}^{2B} \log \frac{e^{\text{sim}(n_i, n_i^+) \cdot e^\tau}}{\sum_{j \in [2B] \setminus \{i\}} e^{\text{sim}(n_i, n_j) \cdot e^\tau}}, \quad (2)$$

where  $\tau$  means the learnable temperature and  $\text{sim}(a, b) = a^\top b / (\|a\| \|b\|)$ .  $\mathcal{L}(\pi, \mu)$  means that we only update the connector  $C_\pi$  and LLMs  $LLM_\mu$ , while keep the vision encoder  $V_\theta$  frozen, aiming for the larger batch size and better performance [22].

## 2.2 Datasets and Experimental Settings

**Datasets.** We obtain a real-world multimodal I2I dataset from our platform. We create the training dataset by randomly choosing related note pairs from user behaviour data gathered over two weeks. One-tenth of pairs in this training dataset is used for the validation set. Next, we randomly select notes from the upcoming week to form the note pool of testing set, excluding any notes that are already in the training dataset. Then, we count the related note pairs in the note pool of testing set. The training dataset contains 1.5M notes and 1.1M note pairs. The testing dataset contains 0.5M notes and 21K note pairs. We provide detailed statistics of the training and testing dataset in Appendix C.

To better evaluate the multimodal representation ability of MLRMs rather than relying heavily on the text modality, we collect pairs that include short notes in the test dataset. We define notes with a token length of less than 50 as short notes, which approximately constitute 10% of the total test notes. We categorize pairs with short query notes as short query pairs and those with short target notes as short target pairs. In the test dataset, the number of short query pairs is 5,620 and the number of short target pairs is 5,582.

**Experimental settings.** In related note pair construction, we set the upper bound of the co-occurrence score *up* as 30 and the lower bound *low* as 0.01. And we set *t* as 3. To maintain context length restrictions, we truncate the titles exceeding 20 tokens, and truncate the contents exceeding 80 tokens. In the fine-tuned experiments, for fair comparison, we add a linear projector to diminish the dimension of note embeddings to 64. The batch size *B* is set to 128<sup>1</sup>. Each batch contains 256 notes. The temperature  $\tau$  is initialized as 3. We provide more training details in Appendix D.

To evaluate the representation ability of MLRMs, we rank all notes in the note pool, excluding the query note, according to the content of query note. We compute recall scores based on the position of the target note in the ranked list. We report Recall@100, Recall@1k and Recall@10k on all pairs, short query pairs and short target pairs in the test dataset.

Table 1: Representation performance of different models (%).

Method	Input	All Pair			Short Query Pair			Short Target Pair		
		R@100	R@1k	R@10k	R@100	R@1k	R@10k	R@100	R@1k	R@10k
<b>Unimodal Training</b>										
CLIP ViT-B	Image	23.21	45.44	71.16	25.24	49.40	75.99	25.58	50.28	75.80
BM25	Text	55.20	72.67	82.83	35.82	48.42	59.71	35.07	49.63	63.68
RoBERTa-wwm-ext	Text	67.59	85.06	93.86	41.23	58.61	76.40	41.80	60.65	80.04
Tomato	Text	71.01	87.38	95.19	43.55	60.70	79.10	45.04	63.45	83.24
Tomato + NoteLLM	Text	71.42	87.78	95.57	44.13	61.86	80.07	45.73	64.28	84.22
Qwen-Chat	Text	73.03	88.41	97.50	45.52	62.21	79.93	46.42	64.49	83.62
<b>Multimodal Training</b>										
METER Merge-attn	Multimodal	68.22	88.37	97.48	50.37	75.61	93.59	50.05	76.55	94.67
METER Co-attn	Multimodal	70.90	89.75	97.88	52.70	78.14	94.65	53.17	79.74	95.65
BLIP-2	Multimodal	68.38	88.22	97.44	52.97	77.83	94.40	54.00	79.74	95.29
MTomato-Base	Multimodal	71.94	88.22	96.13	44.77	63.77	83.31	45.83	66.08	87.02
MQwen-Base	Multimodal	74.02	89.65	97.22	48.15	68.35	88.22	49.82	70.91	91.43
MQwen-bigG	Multimodal	77.64	92.89	98.91	57.45	80.92	95.73	57.90	83.49	96.99
Qwen-VL-Chat <sup>2</sup>	Multimodal	<b>78.54</b>	<b>93.77</b>	<b>99.03</b>	<b>60.43</b>	<b>83.26</b>	<b>96.60</b>	<b>61.63</b>	<b>85.48</b>	<b>97.89</b>

### 2.3 Performance of Multimodal Representation of Fine-tuned MLRMs

We conduct zero-shot experiments on several existing MLLMs in Appendix G, and find that zero-shot is insufficient to adapt MLLMs to representation tasks, performing inferiorly compared to a simple baseline, BM25 [40]. This is due to the misalignment between pre-training tasks and representation tasks [60, 19]. Hence, fine-tuning MLLMs for representation tasks is necessary.

We design three end-to-end MLRMs to examine the representation training method: **MTomato-Base** uses Tomato (our continually pre-trained LLM based on LLaMA 2 [47], which lacks vision perception ability) as the LLM, CLIP ViT-B [37] as the vision encoder and a randomly initialized Q-Former [25] as the connector for efficiency. **MQwen-Base** replaces Tomato with Qwen-Chat [2] in MTomato-Base. **MQwen-bigG** replaces CLIP ViT-B with ViT-bigG [17] in MQwen-Base. We set the visual embedding length of these models as 16 for efficiency. For comparison, we choose two pre-trained MLLMs: **BLIP-2** and **Qwen-VL-Chat** [3]. All vision encoders in these models are frozen for the larger batch size. In addition to MLRMs, we also compare other existing multimodal representation baselines. We provide details about baselines and MLRMs in Appendix E.

The results are shown in Table 1. Several interesting observations can be made. Firstly, MLRMs based on LLMs can outperform existing baselines significantly. Qwen-VL-Chat achieves a 10.78% improvement in R@100 compared to the traditional method, METER Co-attn on all pairs. Secondly, the end-to-end training representation method can enhance the model’s multimodal representation

<sup>1</sup>We train models on 8 × 80GB Nvidia A100 GPUs and the batch size per each GPU is 16.

<sup>2</sup>Due to Qwen-VL-Chat having 256 visual embeddings per image, this model is trained on 32 × 80GB Nvidia A100 GPUs and the batch size per each GPU is 4.

ability. MQwen-bigG improves R@100 on all pairs by 6.31% compared to Qwen-Chat. However, when the visual encoder is small, such as CLIP ViT-B, the enhancement in multimodal perception is not substantial. MTomato-Base only improves R@100 on all pairs by 1.31% compared to Tomato, and MQwen-Base only improves R@100 on all pairs by 1.36% compared to Qwen-Chat. Lastly, although MQwen-bigG is more efficient than Qwen-VL-Chat, which uses the same vision encoder and LLM (see Appendix E.3), there remains a performance gap.

Table 2: Representation performance of fine-tuned MLRMs under different modal inputs (%).

Method	Input	All Pair			Short Query Pair			Short Target Pair		
		R@100	R@1k	R@10k	R@100	R@1k	R@10k	R@100	R@1k	R@10k
<b>Multimodal Training</b>										
BLIP-2	Image	24.72	45.21	69.68	26.07	48.78	75.59	27.59	49.78	75.97
	Text	56.85	75.56	88.26	32.85	47.28	64.66	34.88	51.68	72.98
	Multimodal	68.38	88.22	97.44	52.97	77.83	94.40	54.00	79.74	95.29
MTomato-Base	Image	0.60	1.49	6.98	0.54	1.51	9.15	0.84	2.13	9.70
	Text	71.49	87.59	95.31	43.80	61.74	79.26	44.72	63.89	83.26
	Multimodal	71.94	88.22	96.13	44.77	63.77	83.31	45.83	66.08	87.02
MQwen-Base	Image	1.92	6.59	23.43	2.86	8.54	28.83	3.05	9.38	29.72
	Text	73.14	88.35	95.34	44.50	61.59	78.78	46.12	64.41	83.97
	Multimodal	74.02	89.65	97.22	48.15	68.35	88.22	49.82	70.91	91.43
MQwen-bigG	Image	18.32	38.50	64.56	19.76	41.56	71.32	21.30	42.72	71.54
	Text	70.63	86.09	93.81	39.94	55.77	72.17	43.03	60.02	79.77
	Multimodal	77.64	92.89	98.91	57.45	80.92	95.73	57.90	83.49	96.99
Qwen-VL-Chat	Image	24.67	45.51	70.08	25.94	48.32	75.32	26.94	49.59	75.67
	Text	71.44	86.78	94.43	42.55	58.59	75.86	43.97	61.11	80.17
	Multimodal	78.54	93.77	99.03	60.43	83.26	96.60	61.63	85.48	97.89

We also evaluate all fine-tuned MLRMs under different modal inputs, as shown in Table 2. Firstly, we observe that MTomato-Base and MQwen-Base hardly represent the image content when the input consists solely of images, which shows ignoring visual information. Owing to its more robust vision encoder, MQwen-bigG exhibits superior vision representation capabilities. However, its performance still falls short when compared to BLIP-2 and Qwen-VL-Chat, both of which have undergone multimodal pre-training.

## 2.4 Exploring the Bias of Fine-tuned MLRMs

To further mine the bias in fine-tuned MLRMs, we explore the attention patterns of two modality tokens in different LLMs’ layers. Following [48], we adopt saliency scores to analyze the interaction between the compressed word and two modality tokens in the attention matrices. We randomly select 10,000 notes in batches from the training dataset to count the saliency scores, and compute the saliency scores as follows:

$$I_l = \sum_h \left| A_{h,l}^\top \frac{\partial \mathcal{L}}{\partial A_{h,l}} \right|, \quad (3)$$

where  $A_{h,l}$  means the attention matrix value of the  $h$ -th attention head in the  $l$ -th layer and  $\mathcal{L}$  is the contrastive loss. We sum all attention heads to obtain the saliency matrix  $I_l$  of  $l$ -th layer.  $I_l(i, j)$  means the significance of the information flow from the  $j$ -th word to the  $i$ -th word. To analyze different modality importances for the compressed word, we separate  $I_l$  into three parts as following:  $S_v$ , the mean significance of information flow from the vision embeddings  $E_v$  to the final compressed position  $c$ .  $S_t$ , the mean significance of information flow from the textual embeddings  $E_t$  to the final compressed position  $c$ .  $S_o$ , the mean significance of information flow amongst all words, excluding influences represented by  $S_v$  and  $S_t$ . We provide a more clear formal definition in Appendix F.1.

The results of three parts from the saliency matrix are shown in Figure 3. MLRMs trained end-to-end without pre-training exhibit a low  $S_v$  and a high  $S_o$  in shallow layers, while pre-trained MLLMs, BLIP-2 and Qwen-VL-Chat (see Appendix F.2), have more balanced  $S_v$  and  $S_o$  in shallow layers. This indicates that end-to-end trained MLRMs primarily utilize the information gain from multimodal data to enhance the information flow in the context. Images in these models primarily assist the information flow in identifying crucial information [44, 43], rather than being directly aggregated by representations. Besides, text information flow significantly surpasses visual information flow in end-to-end trained MLRMs.

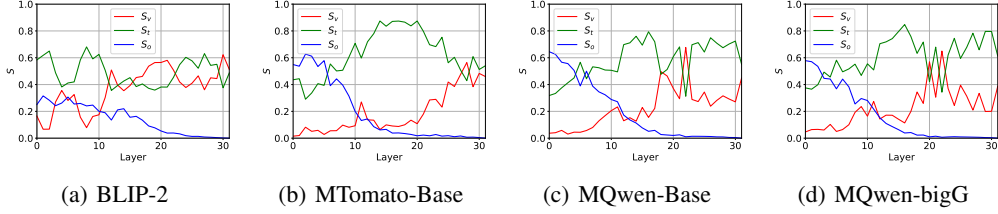


Figure 3: Relative sizes of  $S_v$ ,  $S_t$  and  $S_o$  in different layers of different MLRMs.

### 3 Methodology

From our investigation, MLRMs trained end-to-end without pre-training are suboptimal, primarily due to the disregard of visual information after processing by LLMs. Therefore, we aim to design mechanisms that focus more on visual signals. We propose a novel training framework, **NoteLLM-2**, which contains two methods from different perspectives. The first one is from the prompt viewpoint, called mICL. This method alters the prompt to adjust the attention patterns towards visual information. The second one is from the model architecture perspective, which combines the late fusion with the visual prompt. This enhances the impact of the visual information flow on the final representation by delaying the fusion of visual information. The improved overall framework is shown in Figure 2 (b).

Specifically, given note  $n_i$ , the mICL mechanism does not attempt to compress the multimodal information into one compressed word. Instead, we separate the multimodal note into two single-modality notes. We then adopt a similar ICL way [12, 48] to aggregate the multimodal information. We reformulate our note compression prompt as follows:

**mICL Note Compression Prompt.**

Note content: { 'image': <IMG> }, Compress this note into one word: "<IMG\_EMB>". Note content: { 'title':  $t_i$ , 'topic':  $tp_i$ , 'content':  $ct_i$  }. Compress this note into one word:"

In this template, <IMG\_EMB> is a special token.

After processing the multimodal embeddings with LLMs, we choose relevant hidden states to represent notes. Following [60, 19], we take the previous hidden state of the token <IMG\_EMB> as the visual note representation, denoted as  $\mathbf{n}_i^v$ . Due to the causal attention,  $\mathbf{n}_i^v$  only contains the note image information. We also take the last hidden state as the multimodal note representation, denoted as  $\mathbf{n}_i^m$ , which can compress visual and textual information. This method separates the original single embedding into two modality note embeddings. The multimodal note representation  $\mathbf{n}_i^m$  aggregates useful visual information in a similar manner to ICL.

The late fusion mechanism adopts original visual embedding to enhance the note embeddings. This prevents a textual bias due to the space of LLMs [62] and incorporates more original visual information. Specifically, after extracting image features by the vision encoder  $V_\theta$ , we take the visual feature, which contains the entire image information, such as the [CLS] token in CLIP ViT-B. Then, we use a linear layer to transform these features into the dimension of LLMs, denoted as  $\mathbf{v} \in \mathbb{R}^{h_t}$ . We adopt the same gate mechanism to fuse the original visual information into the two note embeddings.

$$\mathbf{z} = \text{sigmoid}(\mathbf{W}[\mathbf{v}, \mathbf{n}_i^v] + \mathbf{b}),$$

$$\hat{\mathbf{n}}_i^v = \mathbf{z} \odot \mathbf{v} + (\mathbf{1} - \mathbf{z}) \odot \mathbf{n}_i^v,$$
(4)

$$\mathbf{z} = \text{sigmoid}(\mathbf{W}[\mathbf{v}, \mathbf{n}_i^m] + \mathbf{b}),$$

$$\hat{\mathbf{n}}_i^m = \mathbf{z} \odot \mathbf{v} + (\mathbf{1} - \mathbf{z}) \odot \mathbf{n}_i^m,$$
(5)

where  $\hat{\mathbf{n}}_i^v$  and  $\hat{\mathbf{n}}_i^m$  means the fused note embeddings.  $[\cdot, \cdot]$  means the concatenate operation, and  $\mathbf{W}$  and  $\mathbf{b}$  are learnable parameters.  $\odot$  is the element-wise product.

Next, we adopt the two fused embeddings to conduct contrastive learning as follows:

$$\mathcal{L}^v(\pi, \mu) = -\frac{1}{2B} \sum_{i=1}^{2B} \log \frac{e^{\text{sim}(\hat{\mathbf{n}}_i^v, \hat{\mathbf{n}}_i^{v,+}) \cdot e^\tau}}{\sum_{j \in [2B] \setminus \{i\}} e^{\text{sim}(\hat{\mathbf{n}}_i^v, \hat{\mathbf{n}}_j^v) \cdot e^\tau}},$$
(6)

$$\mathcal{L}^m(\pi, \mu) = -\frac{1}{2B} \sum_{i=1}^{2B} \log \frac{e^{\text{sim}(\hat{\mathbf{n}}_i^m, \hat{\mathbf{n}}_i^{m,+}) \cdot e^\tau}}{\sum_{j \in [2B] \setminus \{i\}} e^{\text{sim}(\hat{\mathbf{n}}_i^m, \hat{\mathbf{n}}_j^m) \cdot e^\tau}}, \quad (7)$$

where  $\mathcal{L}^v(\pi, \mu)$  is the loss from visual note embeddings and  $\mathcal{L}^m(\pi, \mu)$  is the loss from the multimodal note embeddings. The final loss is computed as follows:

$$\mathcal{L}^f(\pi, \mu) = \frac{\mathcal{L}^v(\pi, \mu) + \alpha \mathcal{L}^m(\pi, \mu)}{1 + \alpha}, \quad (8)$$

where  $\mathcal{L}^f(\pi, \mu)$  is the final loss and  $\alpha$  is a hyperparameter. In the evaluation, we use  $\hat{\mathbf{n}}_i^m$  as the note embeddings, which contain multimodal information.

## 4 Experiments

Table 3: Performance of NoteLLM-2 based on three different MLRMs (%).

Method	All Pair			Short Query Pair			Short Target Pair		
	R@100	R@1k	R@10k	R@100	R@1k	R@10k	R@100	R@1k	R@10k
MTomato-Base	71.94	88.22	96.13	44.77	63.77	83.31	45.83	66.08	87.02
+ mICL	74.16	90.95	98.26	51.56	75.86	93.84	52.71	78.12	<b>95.82</b>
+ late fusion	74.51	91.37	98.45	54.19	78.02	94.50	54.00	79.71	95.80
+ NoteLLM-2	<b>74.61</b>	<b>91.50</b>	<b>98.47</b>	<b>54.87</b>	<b>78.81</b>	<b>94.69</b>	<b>54.52</b>	79.75	95.46
only late fusion	74.22	91.25	98.43	53.21	77.75	94.65	53.65	<b>79.77</b>	95.59
MQwen-Base	74.02	89.65	97.22	48.15	68.35	88.22	49.82	70.91	91.43
+ mICL	75.82	91.57	98.55	53.32	76.40	94.38	54.52	79.31	96.05
+ late fusion	75.92	91.49	98.28	52.74	76.03	93.65	54.06	78.89	95.53
+ NoteLLM-2	<b>76.50</b>	<b>92.18</b>	<b>98.58</b>	<b>55.72</b>	<b>78.91</b>	<b>94.94</b>	<b>56.13</b>	<b>80.65</b>	<b>96.24</b>
only late fusion	75.84	91.49	98.35	53.36	76.23	93.57	54.27	78.39	95.30
MQwen-bigG	77.64	92.89	98.91	57.45	80.92	95.73	57.90	83.49	96.99
+ mICL	<b>77.97</b>	93.19	<b>98.92</b>	<b>58.50</b>	<b>82.08</b>	<b>96.66</b>	58.58	<b>84.01</b>	<b>97.20</b>
+ late fusion	77.43	92.92	98.78	57.47	81.77	95.89	58.50	83.99	97.16
+ NoteLLM-2	77.56	<b>93.38</b>	98.82	57.94	81.98	96.29	<b>58.79</b>	83.87	97.05
only late fusion	76.24	92.31	98.67	55.21	79.22	95.58	55.15	81.13	96.70

### 4.1 Performance Evaluation

We conduct experiments on all components of NoteLLM-2 based on three MLRMs to show our method effectiveness. Besides, we perform an ablation study, **only late fusion**, which only use late fusion to integrate image and text information, without inputting image embeddings into LLMs.

The results are presented in Table 3. Firstly, NoteLLM-2 can significantly enhance the overall performance for MTomato-Base and MQwen-Base, which have relatively small vision encoders. Additionally, NoteLLM-2 primarily enhances MQwen-bigG in terms of short pairs. Secondly, mICL enhances the performance of all models, while late fusion is more effective in models with relatively small vision encoders. Concurrently, we find that only late fusion is a straightforward and efficient fusion method. However, its simplicity could potentially be a drawback when the vision encoder is more powerful, as it may not fully and effectively interact with LLMs, leading to a loss in performance. Lastly, MQwen-bigG + NoteLLM-2 still underperforms compared to Qwen-VL-Chat, especially in shorter pairs. We attribute this to the significant difference in visual token length between MQwen-bigG (16) and Qwen-VL-Chat (256).

### 4.2 Saliency Scores of Enhanced MLRMs

To further understand the impact of NoteLLM-2 on MLRMs, we illustrate the difference in saliency scores of enhanced MLRMs. The saliency scores for the original fine-tuned method are  $S_v$ ,  $S_t$  and  $S_o$ . The saliency scores for the enhanced fine-tuned method are  $\hat{S}_v$ ,  $\hat{S}_t$  and  $\hat{S}_o$ . We consider the visual note compressed word as a part of the vision embeddings  $E_v$ . Our results are shown in Figure 4. The representations of all enhanced MLRMs amplify the direct focus on images while reducing the emphasis on  $S_o$  in the shallow layers. At the same time,  $S_t$  remains virtually unchanged. This is attributed to mICL’s use of the same compressed prompt to compress both modalities. By

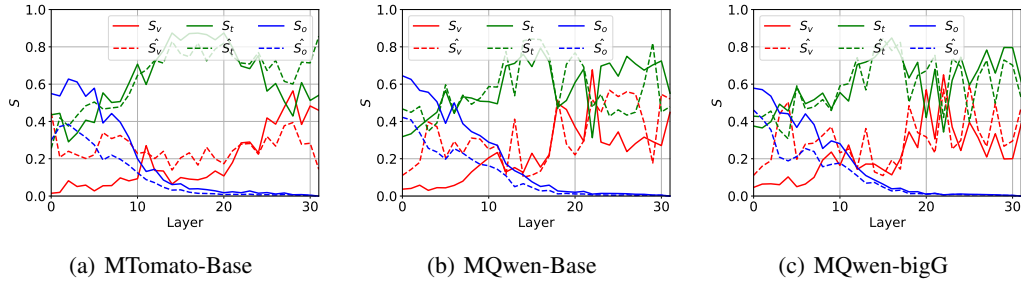


Figure 4: Relative sizes of saliency scores in different layers of different MLRMs.

identifying similar compression patterns from image information, mICL can bolster the concentration of multimodal representations on images, similar to ICL [48].

Table 4: Impact of the number of visual tokens  $L$  (%).

#Visual Tokens	All Pair			Short Query Pair			Short Target Pair		
	R@100	R@1k	R@10k	R@100	R@1k	R@10k	R@100	R@1k	R@10k
8	74.17	90.85	98.16	52.80	76.13	93.76	53.19	77.87	94.48
16	<b>74.61</b>	91.50	98.47	<b>54.87</b>	78.81	94.69	<b>54.52</b>	79.75	95.46
32	74.55	91.41	98.38	54.56	<b>78.91</b>	94.94	54.21	79.83	95.63
48	74.30	<b>91.57</b>	<b>98.48</b>	54.31	78.83	<b>95.13</b>	53.73	<b>80.06</b>	<b>95.92</b>

Table 5: Impact of textual loss and visual loss ratio  $\alpha$  (%).

$\alpha$	All Pair			Short Query Pair			Short Target Pair		
	R@100	R@1k	R@10k	R@100	R@1k	R@10k	R@100	R@1k	R@10k
1	73.94	91.11	98.38	54.13	78.16	94.67	54.06	79.00	95.38
3	74.38	91.41	98.42	54.15	77.71	94.59	54.06	79.31	<b>95.53</b>
9	<b>74.61</b>	<b>91.50</b>	98.47	<b>54.87</b>	<b>78.81</b>	94.69	<b>54.52</b>	79.75	95.46
19	74.53	91.33	<b>98.54</b>	54.56	78.68	<b>95.00</b>	53.92	<b>80.04</b>	<b>95.53</b>

### 4.3 Hyper-Parameter Analysis

In this section, we use MTomato-Base to conduct hyper-parameter analysis experiments.

**Impact of length of visual tokens.** We explore the impact of visual token length. The results are shown in Table 4. Reducing the length from 16 to 8 worsens performance in short pairs. There exists a tradeoff between performance and inference speed concerning the length of visual tokens.

**Impact of text and visual loss ratio.** We vary the ratio of text to visual loss  $\alpha$ , as shown in Table 5. When the ratio is small, the performance is slightly worse. However, as we increase the ratio, we find that our method is insensitive to changes in the text to visual loss ratio.

## 5 Conclusion

This paper explores using LLMs to improve textual comprehension in multimodal representation tasks under I2I recommendation scenarios. We design an end-to-end training method that can customize the integration of any existing LLMs and vision encoders. This approach reduces reliance on open-source MLLMs, which require costly multimodal pre-training. To prevent the problem of ignoring visual information in end-to-end training, we propose NoteLLM-2, which contains mICL and late fusion. The effectiveness of this approach is confirmed through extensive experiments.

## References

- [1] Llama3. <https://llama.meta.com/llama3/>.
- [2] Jinze Bai, Shuai Bai, Yunfei Chu, Zeyu Cui, Kai Dang, Xiaodong Deng, Yang Fan, Wenbin Ge, Yu Han, Fei Huang, et al. 2023. Qwen technical report. *arXiv preprint arXiv:2309.16609*.
- [3] Jinze Bai, Shuai Bai, Shusheng Yang, Shijie Wang, Sinan Tan, Peng Wang, Junyang Lin, Chang Zhou, and Jingren Zhou. 2023. Qwen-vl: A frontier large vision-language model with versatile abilities. *arXiv preprint arXiv:2308.12966*.
- [4] Parishad BehnamGhader, Vaibhav Adlakha, Marius Mosbach, Dzmitry Bahdanau, Nicolas Chapados, and Siva Reddy. 2024. Llm2vec: Large language models are secretly powerful text encoders. *arXiv preprint arXiv:2404.05961*.
- [5] Yunkai Chen, Qimeng Wang, Shiwei Wu, Yan Gao, Tong Xu, and Yao Hu. 2024. TOMGPT: Reliable Text-Only Training Approach for Cost-Effective Multi-modal Large Language Model. *TKDD*.
- [6] Zhihong Chen, Guiming Chen, Shizhe Diao, Xiang Wan, and Benyou Wang. 2023. On the Difference of BERT-style and CLIP-style Text Encoders. In *Findings of ACL*, pages 13710–13721.
- [7] Wei-Lin Chiang, Zhuohan Li, Zi Lin, Ying Sheng, Zhanghao Wu, Hao Zhang, Lianmin Zheng, Siyuan Zhuang, Yonghao Zhuang, Joseph E. Gonzalez, Ion Stoica, and Eric P. Xing. 2023. Vicuna: An Open-Source Chatbot Impressing GPT-4 with 90%\* ChatGPT Quality.
- [8] Junyoung Chung, Caglar Gulcehre, KyungHyun Cho, and Yoshua Bengio. 2014. Empirical evaluation of gated recurrent neural networks on sequence modeling. *arXiv preprint arXiv:1412.3555*.
- [9] Yiming Cui, Wanxiang Che, Ting Liu, Bing Qin, and Ziqing Yang. 2021. Pre-training with whole word masking for chinese bert. *IEEE/ACM Transactions on Audio, Speech, and Language Processing*, 29:3504–3514.
- [10] Nilotpal Das, Aniket Joshi, Promod Yenigalla, and Gourav Agrwal. 2022. MAPS: multimodal attention for product similarity. In *WACV*, pages 3338–3346.
- [11] DeepSeek-AI. 2024. DeepSeek-V2: A Strong, Economical, and Efficient Mixture-of-Experts Language Model.
- [12] Qingxiu Dong, Lei Li, Damai Dai, Ce Zheng, Zhiyong Wu, Baobao Chang, Xu Sun, Jingjing Xu, and Zhifang Sui. 2022. A survey on in-context learning. *arXiv preprint arXiv:2301.00234*.
- [13] Runpei Dong, Chunrui Han, Yuang Peng, Zekun Qi, Zheng Ge, Jinrong Yang, Liang Zhao, Jianjian Sun, Hongyu Zhou, Haoran Wei, et al. 2023. DreamLLM: Synergistic Multimodal Comprehension and Creation. In *The Twelfth International Conference on Learning Representations*.
- [14] Zi-Yi Dou, Yichong Xu, Zhe Gan, Jianfeng Wang, Shuohang Wang, Lijuan Wang, Chenguang Zhu, Pengchuan Zhang, Lu Yuan, Nanyun Peng, et al. 2022. An empirical study of training end-to-end vision-and-language transformers. In *CVPR*, pages 18166–18176.
- [15] Yuying Ge, Sijie Zhao, Ziyun Zeng, Yixiao Ge, Chen Li, Xintao Wang, and Ying Shan. 2023. Planting a SEED of Vision in Large Language Model. In *ICLR*.
- [16] Xiao Han, Xiatian Zhu, Licheng Yu, Li Zhang, Yi-Zhe Song, and Tao Xiang. 2023. Famevil: Multi-tasking vision-language model for heterogeneous fashion tasks. In *CVPR*, pages 2669–2680.
- [17] Gabriel Ilharco, Mitchell Wortsman, Ross Wightman, Cade Gordon, Nicholas Carlini, Rohan Taori, Achal Dave, Vaishaal Shankar, Hongseok Namkoong, John Miller, Hannaneh Hajishirzi, Ali Farhadi, and Ludwig Schmidt. 2021. OpenCLIP. If you use this software, please cite it as below.

- [18] Albert Q Jiang, Alexandre Sablayrolles, Arthur Mensch, Chris Bamford, Devendra Singh Chaplot, Diego de las Casas, Florian Bressand, Gianna Lengyel, Guillaume Lample, Lucile Saulnier, et al. 2023. Mistral 7B. *arXiv preprint arXiv:2310.06825*.
- [19] Ting Jiang, Shaohan Huang, Zhongzhi Luan, Deqing Wang, and Fuzhen Zhuang. 2023. Scaling sentence embeddings with large language models. *arXiv preprint arXiv:2307.16645*.
- [20] Yang Jin, Yongzhi Li, Zehuan Yuan, and Yadong Mu. 2023. Learning Instance-Level Representation for Large-Scale Multi-Modal Pretraining in E-commerce. In *CVPR*, pages 11060–11069.
- [21] Jeff Johnson, Matthijs Douze, and Hervé Jégou. 2019. Billion-scale similarity search with GPUs. *IEEE Transactions on Big Data*, 7(3):535–547.
- [22] Siddharth Karamcheti, Suraj Nair, Ashwin Balakrishna, Percy Liang, Thomas Kollar, and Dorsa Sadigh. 2024. Prismatic vlms: Investigating the design space of visually-conditioned language models. *arXiv preprint arXiv:2402.07865*.
- [23] Jacob Devlin Ming-Wei Chang Kenton and Lee Kristina Toutanova. 2019. BERT: Pre-training of Deep Bidirectional Transformers for Language Understanding. In *NAACL*, pages 4171–4186.
- [24] Hugo Laurençon, Léo Tronchon, Matthieu Cord, and Victor Sanh. 2024. What matters when building vision-language models? *arXiv preprint arXiv:2405.02246*.
- [25] Junnan Li, Dongxu Li, Silvio Savarese, and Steven Hoi. 2023. Blip-2: Bootstrapping language-image pre-training with frozen image encoders and large language models. In *ICML*, pages 19730–19742. PMLR.
- [26] Junnan Li, Dongxu Li, Caiming Xiong, and Steven Hoi. 2022. Blip: Bootstrapping language-image pre-training for unified vision-language understanding and generation. In *ICML*, pages 12888–12900. PMLR.
- [27] Junnan Li, Ramprasaath Selvaraju, Akhilesh Gotmare, Shafiq Joty, Caiming Xiong, and Steven Chu Hong Hoi. 2021. Align before fuse: Vision and language representation learning with momentum distillation. *NeurIPS*, 34:9694–9705.
- [28] Bin Lin, Bin Zhu, Yang Ye, Munan Ning, Peng Jin, and Li Yuan. 2023. Video-llava: Learning united visual representation by alignment before projection. *arXiv preprint arXiv:2311.10122*.
- [29] Haotian Liu, Chunyuan Li, Yuheng Li, and Yong Jae Lee. 2023. Improved baselines with visual instruction tuning. *arXiv preprint arXiv:2310.03744*.
- [30] Qidong Liu, Jiayi Hu, Yutian Xiao, Jingtong Gao, and Xiangyu Zhao. 2023. Multimodal recommender systems: A survey. *arXiv preprint arXiv:2302.03883*.
- [31] Xueguang Ma, Liang Wang, Nan Yang, Furu Wei, and Jimmy Lin. 2023. Fine-tuning llama for multi-stage text retrieval. *arXiv preprint arXiv:2310.08319*.
- [32] Muhammad Maaz, Hanoona Rasheed, Salman Khan, and Fahad Shahbaz Khan. 2023. Video-chatgpt: Towards detailed video understanding via large vision and language models. *arXiv preprint arXiv:2306.05424*.
- [33] Brandon McKinzie, Zhe Gan, Jean-Philippe Fauconnier, Sam Dodge, Bowen Zhang, Philipp Dufter, Dhruvi Shah, Xianzhi Du, Futang Peng, Floris Weers, et al. 2024. MM1: Methods, Analysis & Insights from Multimodal LLM Pre-training. *arXiv preprint arXiv:2403.09611*.
- [34] Niklas Muennighoff, Hongjin Su, Liang Wang, Nan Yang, Furu Wei, Tao Yu, Amanpreet Singh, and Douwe Kiela. 2024. Generative representational instruction tuning. *arXiv preprint arXiv:2402.09906*.
- [35] Niklas Muennighoff, Nouamane Tazi, Loïc Magne, and Nils Reimers. 2022. MTEB: Massive Text Embedding Benchmark. *arXiv preprint arXiv:2210.07316*.
- [36] Arvind Neelakantan, Tao Xu, Raul Puri, Alec Radford, Jesse Michael Han, Jerry Tworek, Qiming Yuan, Nikolas Tezak, Jong Wook Kim, Chris Hallacy, et al. 2022. Text and code embeddings by contrastive pre-training. *arXiv preprint arXiv:2201.10005*.

- [37] Alec Radford, Jong Wook Kim, Chris Hallacy, Aditya Ramesh, Gabriel Goh, Sandhini Agarwal, Girish Sastry, Amanda Askell, Pamela Mishkin, Jack Clark, et al. 2021. Learning transferable visual models from natural language supervision. In *ICML*, pages 8748–8763. PMLR.
- [38] Jeff Rasley, Samyam Rajbhandari, Olatunji Ruwase, and Yuxiong He. 2020. Deepspeed: System optimizations enable training deep learning models with over 100 billion parameters. In *KDD*, pages 3505–3506.
- [39] Jie Ren, Samyam Rajbhandari, Reza Yazdani Aminabadi, Olatunji Ruwase, Shuangyan Yang, Minjia Zhang, Dong Li, and Yuxiong He. 2021. {Zero-offload}: Democratizing {billion-scale} model training. In *USENIX Annual Technical Conference*, pages 551–564.
- [40] Stephen Robertson, Hugo Zaragoza, et al. 2009. The probabilistic relevance framework: BM25 and beyond. *Foundations and Trends® in Information Retrieval*, 3(4):333–389.
- [41] Jacob Mitchell Springer, Suhas Kotha, Daniel Fried, Graham Neubig, and Aditi Raghunathan. 2024. Repetition Improves Language Model Embeddings. *arXiv preprint arXiv:2402.15449*.
- [42] Yixuan Su, Tian Lan, Huayang Li, Jialu Xu, Yan Wang, and Deng Cai. 2023. Pandagpt: One model to instruction-follow them all. *arXiv preprint arXiv:2305.16355*.
- [43] Lin Sun, Jiquan Wang, Yindu Su, Fangsheng Weng, Yuxuan Sun, Zengwei Zheng, and Yuanyi Chen. 2020. RIVA: a pre-trained tweet multimodal model based on text-image relation for multimodal NER. In *COLING*, pages 1852–1862.
- [44] Lin Sun, Jiquan Wang, Kai Zhang, Yindu Su, and Fangsheng Weng. 2021. RpBERT: a text-image relation propagation-based BERT model for multimodal NER. In *AAAI*, volume 35, pages 13860–13868.
- [45] Quan Sun, Yuxin Fang, Ledell Wu, Xinlong Wang, and Yue Cao. 2023. Eva-clip: Improved training techniques for clip at scale. *arXiv preprint arXiv:2303.15389*.
- [46] Quan Sun, Jinsheng Wang, Qiyong Yu, Yufeng Cui, Fan Zhang, Xiaosong Zhang, and Xinlong Wang. 2024. EVA-CLIP-18B: Scaling CLIP to 18 Billion Parameters. *arXiv preprint arXiv:2402.04252*.
- [47] Hugo Touvron, Louis Martin, Kevin Stone, Peter Albert, Amjad Almahairi, Yasmine Babaei, Nikolay Bashlykov, Soumya Batra, Prajjwal Bhargava, Shruti Bhosale, et al. 2023. Llama 2: Open foundation and fine-tuned chat models. *arXiv preprint arXiv:2307.09288*.
- [48] Lean Wang, Lei Li, Damai Dai, Deli Chen, Hao Zhou, Fandong Meng, Jie Zhou, and Xu Sun. 2023. Label Words are Anchors: An Information Flow Perspective for Understanding In-Context Learning. In *EMNLP*, pages 9840–9855.
- [49] Wenhui Wang, Hangbo Bao, Li Dong, Johan Bjorck, Zhiliang Peng, Qiang Liu, Kriti Aggarwal, Owais Khan Mohammed, Saksham Singhal, Subhojit Som, et al. 2023. Image as a foreign language: Beit pretraining for vision and vision-language tasks. In *CVPR*, pages 19175–19186.
- [50] Yinwei Wei, Xiang Wang, Liqiang Nie, Xiangnan He, Richang Hong, and Tat-Seng Chua. 2019. MMGCN: Multi-modal graph convolution network for personalized recommendation of micro-video. In *MM*, pages 1437–1445.
- [51] Chuhan Wu, Fangzhao Wu, Tao Qi, Chao Zhang, Yongfeng Huang, and Tong Xu. 2022. Mm-rec: Visiolinguistic model empowered multimodal news recommendation. In *SIGIR*, pages 2560–2564.
- [52] Derong Xu, Wei Chen, Wenjun Peng, Chao Zhang, Tong Xu, Xiangyu Zhao, Xian Wu, Yefeng Zheng, and Enhong Chen. 2023. Large language models for generative information extraction: A survey. *arXiv preprint arXiv:2312.17617*.
- [53] Jiahao Xun, Shengyu Zhang, Zhou Zhao, Jieming Zhu, Qi Zhang, Jingjie Li, Xiuqiang He, Xiaofei He, Tat-Seng Chua, and Fei Wu. 2021. Why do we click: visual impression-aware news recommendation. In *MM*, pages 3881–3890.

- [54] Xiaoyong Yang, Yadong Zhu, Yi Zhang, Xiaobo Wang, and Quan Yuan. 2020. Large scale product graph construction for recommendation in e-commerce. *arXiv preprint arXiv:2010.05525*.
- [55] Shukang Yin, Chaoyou Fu, Sirui Zhao, Ke Li, Xing Sun, Tong Xu, and Enhong Chen. 2023. A survey on multimodal large language models. *arXiv preprint arXiv:2306.13549*.
- [56] Jiahui Yu, Zirui Wang, Vijay Vasudevan, Legg Yeung, Mojtaba Seyedhosseini, and Yonghui Wu. 2022. Coca: Contrastive captioners are image-text foundation models. *arXiv preprint arXiv:2205.01917*.
- [57] Licheng Yu, Jun Chen, Animesh Sinha, Mengjiao Wang, Yu Chen, Tamara L Berg, and Ning Zhang. 2022. Commercem: Large-scale commerce multimodal representation learning with omni retrieval. In *KDD*, pages 4433–4442.
- [58] Xiaohua Zhai, Basil Mustafa, Alexander Kolesnikov, and Lucas Beyer. 2023. Sigmoid loss for language image pre-training. In *ICCV*, pages 11975–11986.
- [59] Beichen Zhang, Pan Zhang, Xiaoyi Dong, Yuhang Zang, and Jiaqi Wang. 2024. Long-clip: Unlocking the long-text capability of clip. *arXiv preprint arXiv:2403.15378*.
- [60] Chao Zhang, Shiwei Wu, Haoxin Zhang, Tong Xu, Yan Gao, Yao Hu, and Enhong Chen. 2024. NoteLLM: A Retrievable Large Language Model for Note Recommendation. *arXiv preprint arXiv:2403.01744*.
- [61] Chao Zhang, Zichao Yang, Xiaodong He, and Li Deng. 2020. Multimodal intelligence: Representation learning, information fusion, and applications. *IEEE Journal of Selected Topics in Signal Processing*, 14(3):478–493.
- [62] Yi-Fan Zhang, Weichen Yu, Qingsong Wen, Xue Wang, Zhang Zhang, Liang Wang, Rong Jin, and Tieniu Tan. 2024. Debiasing Large Visual Language Models. *arXiv preprint arXiv:2403.05262*.
- [63] Xiaoyang Zheng, Zilong Wang, Sen Li, Ke Xu, Tao Zhuang, Qingwen Liu, and Xiaoyi Zeng. 2023. Make: Vision-language pre-training based product retrieval in taobao search. In *WWW*, pages 356–360.
- [64] Han Zhu, Xiang Li, Pengye Zhang, Guozheng Li, Jie He, Han Li, and Kun Gai. 2018. Learning tree-based deep model for recommender systems. In *KDD*, pages 1079–1088.

## Appendix

### A Related Work

#### A.1 Multimodal Representation

With the advancement of pre-training techniques, numerous studies utilize web-scale image-text data to pre-train models for a fundamental understanding of multimodal information. There are two main pre-training techniques. The first technique adopts generative pre-training objectives, following masked language/image modeling [14, 49, 27] or image captioning [56, 26]. The second technique uses contrastive pre-training objectives, such as contrastive learning [37, 58, 45, 46, 56, 49] and image-text matching tasks [14, 27, 26]. These models demonstrate a powerful zero-shot ability in many downstream tasks. However, the text comprehension capabilities of these models are unsatisfactory [6, 59], particularly in the era of LLMs. In this work, we explore to use LLMs to enhance the multimodal representations.

#### A.2 Large Language Models

LLMs have attracted extensive attention due to their remarkable text understanding and generation capability [18, 7, 2, 47]. Therefore, numerous text applications have been developed based on LLMs [31, 60, 34, 52, 22]. To understand more modality information, LLMs are extended into MLLMs [3, 5, 55, 33, 24]. Most MLLMs employ specialized modality encoders to capture non-textual information [42, 3, 5]. This information is then mapped into textual LLM space using connectors and subsequently processed by LLMs. Due to the significant understanding ability of LLMs, MLLMs can generate answers according to textual instruction and multimodal information [15, 13, 3, 5]. While existing studies primarily focus on the generation abilities of LLMs, some explore the text representation ability of LLMs [34, 41, 60, 19, 31, 4], demonstrating significant potential to enhance performance for numerous downstream tasks. However, no studies have explored the multimodal representation ability with the assistance of LLMs. Therefore, we aim to investigate the multimodal representation ability enhanced by LLMs in recommendation scenarios.

#### A.3 Multimodal I2I Recommendation

I2I recommendation generates a ranked list of items from a vast pool based on a specific target item, which is an important technique for recall stages in recommendation [54, 64, 60]. I2I recommendation employs either a pre-constructed I2I index [54] or the approximate k-nearest neighbor method [21] to retrieve relevant items online. Some studies have investigated multimodal content-based I2I recommendations [57, 10, 20, 63, 16]. For example, CommerceMM [57] adopts multimodal pre-training tasks used in METER [14] and omni-retrieval tasks to train commerce multimodal representation. MAPS [10] proposes a multimodal attention framework to measure product similarity. However, these works adopt small-scale pre-trained visual-linguistic models as backbones, which have huge potential for scaling up. As shown in [60, 19, 4], LLMs can outperform smaller models in textual representation tasks significantly. Therefore, in this work, we explore empowering the multimodal representations with LLMs in multimodal I2I recommendation.

### B Limitations and Future Works

**More modalities.** In this work, our focus is primarily on the processing of multimodal situations that involve the input of a single image and corresponding text information. This is the most simplified situation within our research scenarios. In fact, the scope of our representation method can extend to include audio and video data [42, 32, 28]. This direction presents an opportunity for further exploration and expansion into more complex modalities.

**General scenarios.** Our MLRMs mainly focus on the multimodal representation ability in recommendation scenarios. These scenarios determine item similarity by analyzing the interaction between items and users. However, this is not a universally applicable scenario. The current focus of our MLRMs is somewhat specialized and may not cover all potential use cases. Given the potential of MLRMs, it is promising to consider broadening their multimodal representation ability into more general scenarios [35].

**Larger and stronger base models.** Due to the rapid development of LLMs and vision encoders, there are an extensive range of larger and more powerful base models available in the market [58, 2, 11]. However, due to resource limitations and the demand for rapid recommendations, we have not yet experimented with all of these models. There is still a vast scope to investigate more advanced models, which could potentially boost performance even further.

## C Dataset Details

Table 6: Detailed statistics of training and testing dataset.

training dataset			
# notes	1,487,613	# note pairs	1,130,906
avg. # words per title	12.38	avg. # topic per note	5.26
avg. # words per topic	4.53	avg. # words per content	133.20
testing dataset			
# notes	534,144	# note pairs	21,262
avg. # words per title	11.68	avg. # topic per note	4.58
avg. # words per topic	4.50	avg. # words per content	116.00

## D Training Details

Table 7: Detailed training hyperparameters for training MLRMs.

Configuration	Hyperparameter
Optimizer	AdamW
$\beta_1$	0.9
$\beta_2$	0.999
$\epsilon$	$1e^{-8}$
Max gradient norm	1.0
Weight decay	$1e^{-3}$
Peak learning rate	$3e^{-6}$
Warmup Ratio	0.1
Learning rate scheduler	linear decay
Numerical precision	bf16
Global batch size	128
Training steps	7,956

For all models with LLMs, we list the detailed training hyperparameter in Table 7. Besides, we use DeepSpeed [38], and Zero Redundancy Optimizer (ZeRO) [39] Stage 3 to train our models.

## E Model Details

### E.1 Baseline Details

To evaluate the effectiveness of MLRMs, we compare them with several baselines. (1) **CLIP ViT-B** [37] is trained using only image input. (2) **BM25** [40] is a basic baseline, which counts the relevance between the query and documents based on every word in the query. (3) **RoBERTa-wwm-ext** [9] is a classic traditional Chinese BERT-like [23] text encoder with pure text input. (4) **Tomato** is our continually pre-trained LLM that is based on LLaMA 2 [47] and utilizes data from our platform for training. (5) **NoteLLM** [60] unifies the embedding generation and topic generation into one task. (6) **METER Merge-attn** and **METER Co-attn** [14] leverage best training strategy to train vision-and-language transformers. METER Merge-attn adopts the merged attention as the fusion module, while METER Co-attn uses co-attention as the fusion module. All baselines are trained on our training dataset.

## E.2 End-to-End MLRM Details

We provide the details in Table 8.

Table 8: Model settings of end-to-end MLRMs.

Configuration	MTomato-Base	MQwen-Base	MQwen-bigG
Vision encoder $V_\theta$ init.	CLIP ViT-B	CLIP ViT-B	OpenCLIP ViT-bigG
Connector $C_\pi$ init.	random Q-Former	random Q-Former	random Q-Former
LLM $LLM_\mu$ init.	Tomato	Qwen-Chat	Qwen-Chat
# Vision encoder layers	12	12	48
# Vision encoder attention heads	12	12	16
Vision encoder sequence length $L$	196	196	256
Vision encoder hidden size $h_v$	768	768	1,664
Vision encoder intermediate size	3,072	3,072	8,192
# Q-Former layers	6	6	6
# Q-Former attention heads	12	12	12
Learnable query numbers $L_c$	16	16	16
Q-Former cross attention frequency	2	2	2
Q-Former cross attention hidden size	768	768	1,664
Q-Former hidden size	768	768	1,536
Q-Former intermediate size	3,072	3,072	3,072
# LLM layers	32	32	32
# LLM attention heads	32	32	32
Vocab size	49,216	151,936	151,936
LLM hidden size $h_t$	4,096	4,096	4,096
LLM intermediate size	11,008	22,016	22,016

## E.3 Comparison of MLRMs

We provide the comparison in Table 9.

Table 9: Comparison of different LLMs for representation tasks.  $L_c$  means the number of vision embeddings for each image. The inference speed test is conducted on an A100 GPU, with an inference batch size set at 50. All notes in this test are the longest note in the dataset. The speed is quantified as the number of longest notes inferred per second.

Method	Vision Encoder	LLM	VL Connector	# Total Par.	$L_c$	Inf. Speed
Tomato	-	Tomato (6.7B)	-	6.7B	-	59.0
Qwen-Chat	-	Qwen-Chat (7.1B)	-	7.1B	-	57.0
BLIP-2	ViT-g (1.0B)	OPT (6.7B)	Q-Former (105.1M)	7.8B	32	44.2
LLaVA-1.5	ViT-L (303.5M)	Vicuna (6.7B)	MLP (21.0M)	7.1B	576	12.1
Qwen-VL-Chat	ViT-bigG (1.8B)	Qwen-Chat (7.1B)	Resamplers (76.1M)	9.0B	256	11.5
MTomato-Base	ViT-B (85.8M)	Tomato (6.7B)	Q-Former (49.6M)	6.8B	16	51.5
+ NoteLLM-2	ViT-B (85.8M)	Tomato (6.7B)	Q-Former (49.6M)	6.9B	16	48.2
MQwen-Base	ViT-B (85.8M)	Qwen-Chat (7.1B)	Q-Former (49.6M)	7.3B	16	50.5
+ NoteLLM-2	ViT-B (85.8M)	Qwen-Chat (7.1B)	Q-Former (49.6M)	7.3B	16	46.9
MQwen-bigG	ViT-bigG (1.8B)	Qwen-Chat (7.1B)	Q-Former (142.9M)	9.1B	16	36.8
+ NoteLLM-2	ViT-bigG (1.8B)	Qwen-Chat (7.1B)	Q-Former (142.9M)	9.2B	16	35.2

## F More Information about Saliency Scores

### F.1 Formal Definition of $S_v$ , $S_t$ and $S_o$

$S_v$ , the mean significance of information flow from the vision embeddings  $E_v$  to the final compressed position  $c$ :

$$S_v = \frac{\sum_{(i,j) \in P_v} I_l(i,j)}{|P_v|}, \quad (9)$$

$$P_v = \{(c, j) : j \in E_v\}.$$

$S_t$ , the mean significance of information flow from the textual embeddings  $E_t$  to the final compressed position  $c$ :

$$S_t = \frac{\sum_{(i,j) \in P_t} I_l(i,j)}{|P_t|}, \quad (10)$$

$$P_t = \{(c, j) : j \in E_t, j < c\}.$$

$S_o$ , the mean significance of information flow amongst all words, excluding influences represented by  $S_v$  and  $S_t$ :

$$S_o = \frac{\sum_{(i,j) \in P_o} I_l(i,j)}{|P_o|}, \quad (11)$$

$$P_o = \{(i, j) : j < i\} - P_v - P_t.$$

## F.2 Results of Qwen-VL-Chat

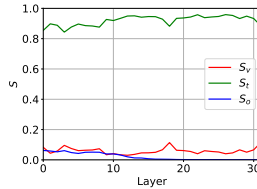


Figure 5: Relative sizes of  $S_v$ ,  $S_t$  and  $S_o$  in different layers of Qwen-VL-Chat.

We observe a unique pattern of saliency scores in Qwen-VL-Chat, as shown in Figure 5. The predominant information flow in Qwen-VL-Chat is textual, with a value higher than 0.8 in all layers. This result is attributed to the extensive visual embeddings (256 in Qwen-VL-Chat) inputted into LLMs, which reduces the average saliency of image information flow. This denotes that traditional MLLMs are not directly suitable for MLRMs. The necessary action to adapt MLLMs to MLRMs is enhancing the efficiency of information flow.

## G Performance of Zero-shot Multimodal Representation

Table 10: Zero-shot representation performance of different models (%).

Method	Input	All Pair			Short Query Pair			Short Target Pair		
		R@100	R@1k	R@10k	R@100	R@1k	R@10k	R@100	R@1k	R@10k
BLIP-2	Image	19.60	34.16	53.49	19.08	34.92	56.18	20.06	36.41	58.20
	Text	15.83	27.29	44.50	9.42	16.36	31.29	12.16	21.15	39.94
	Multimodal	27.28	43.00	62.69	22.46	36.93	59.54	25.16	40.54	60.92
LLaVA-1.5	Image	18.88	33.17	53.14	19.64	34.18	56.18	21.00	35.38	57.10
	Text	30.86	46.71	64.14	21.90	34.43	49.63	22.28	32.98	47.48
	Multimodal	37.01	55.46	73.71	30.51	47.78	<b>68.73</b>	31.56	48.09	68.13
Qwen-VL	Image	17.55	31.62	51.58	17.77	33.55	55.56	18.41	33.88	55.97
	Text	38.74	54.65	70.37	23.31	35.17	51.95	22.17	34.84	51.29
	Multimodal	37.88	55.51	74.73	26.28	43.20	64.89	29.82	47.63	<b>69.72</b>
Qwen-VL-Chat	Image	17.43	31.15	50.48	17.59	32.29	55.04	18.75	33.40	55.09
	Text	37.92	53.02	68.48	22.63	33.87	49.15	21.32	32.50	48.03
	Multimodal	40.93	58.59	75.44	29.10	44.48	64.14	31.81	49.09	68.57
Qwen-Chat	Text	38.98	54.08	69.02	23.08	34.90	50.44	26.04	38.35	53.33
	Tomato	42.67	60.54	78.01	24.51	37.35	56.45	32.27	46.85	66.75
BM25	Text	<b>55.20</b>	<b>72.67</b>	<b>82.83</b>	<b>35.82</b>	<b>48.42</b>	59.71	<b>35.07</b>	<b>49.63</b>	63.68

In this section, we explore the multimodal representation ability of MLLMs in a zero-shot way in the multimodal I2I recommendation task. We select four popular MLLMs, i.e., **BLIP-2** [25], **LLaVA-1.5** [29], **Qwen-VL** [3] and **Qwen-VL-Chat** [3]. We also compare some baselines **BM25** [40], **Qwen-Chat** [2] and our continual pre-trained LLM **Tomato**, which is pre-trained on our platform data based on LLaMA 2 [47], but lacks vision perception ability. The MLLMs details are concluded in Table 9. To understand the representation ability of MLLMs for different modalities, we also input images and texts independently for the representation test.

The results are presented in Table 10. We have several observations. Firstly, the zero-shot representation performance of existing MLLMs is inferior to BM25. This indicates that despite their excellent visual understanding, the zero-shot multimodal representation ability of MLLMs is unsatisfactory. This is because MLLMs are trained using language modeling loss, which mismatches representation tasks. Therefore, additional training is needed to properly align MLLMs with representation tasks. Next, we find that MLLMs can achieve better performance for multimodal input in most cases, which demonstrates that MLLMs can extract and fuse multimodal information effectively. At the same time, we discover that most MLLMs are better at representing text information than image information. This is reasonable because most parameters of MLLMs originate from LLMs, and the text of notes is more discriminative than images in our scenarios. Lastly, we find that LLMs can achieve performance comparable to MLLMs without any image input.

## H Case Study

We show some cases for multimodal I2I note recommendation as shown in Figure 6. In the first case, both the query note and the target note discuss a guide to Oahu, an island in Hawaii. MTomato-Base + NoteLLM-2 successfully ranks the target note in the top position. While METER Co-attn and MTomato-Base also recall relevant notes in the first place, they differ slightly. One talks about an unpleasant experience in Oahu, and the other discusses an overall trip plan for Hawaii. The second example illustrates a note pair about the Pagani car model. Although all baselines recall notes about various car models, these notes discuss many different types of cars. MTomato-Base + NoteLLM-2 ranks the Pagani model car in the first place, which can be attributed to both the image and the text content. The third case discusses how to make good coffee and coffee tricks. LLM-based methods recall relevant notes about the tools needed to make coffee and how to do it. In contrast, METER Co-attn, which has a weaker understanding of text, only recommends coffee beans. The last case involves a short note pair. The query note is about an AI drawing for China’s National Day, and the target note is about a mooncake drawn by AI, which relates to the Chinese traditional festival, the Mid-Autumn Festival. We find that MTomato-Base + NoteLLM-2 can understand the query note image about Chinese culture and recommends notes talking about Chang’e, a figure from Chinese folklore associated with the Mid-Autumn Festival. Tomato and MTomato-Base only focus on the AI painting, rather than the image content.

Query Note	Target Note	METER Co-attn	Tomato	MTomato-Base	MTomato-Base + NoteLLM-2
<p><b>Image:</b> </p> <p><b>Title:</b> From Hawai'i with Love <b>Topic:</b> #Hawaii #Oahu Travel ... <b>Content:</b> I have been thinking about Hawaii for a long time. Finally I found O'ahu where I flew to during my long vacation...</p>	<p><b>Image:</b> </p> <p><b>Title:</b> Hawaiian 0033 <b>Topic:</b> #Hawaii travel #Hawaii Oahu Island Guide ... <b>Content:</b> It's off-season recently, so I finally don't have to queue. I like Honolulu, which is less crowded ...</p>	<p><b>Image:</b> </p> <p><b>Title:</b> Oahu's running account <b>Topic:</b> #Hawaii <b>Content:</b> Going to Oahu from the Big Island suddenly felt like it was no longer fun. I stayed at the Hilton Hawaiian ... <b>Target Ranking:</b> 7th</p>	<p><b>Image:</b> </p> <p><b>Title:</b> Okinawa is the first city I visited in Japan <b>Topic:</b> #Okinawa tour #Okinawa #Travel ... <b>Content:</b> Our tour comes to Okinawa. It's called the Hawaiian Island of the East ... <b>Target Ranking:</b> 8th</p>	<p><b>Image:</b> </p> <p><b>Title:</b> Rainbow Hawaii Weekly itinerary <b>Content:</b> Day 1 O'ahu. Lanai Lookout. Makapu'u Point Lighthouse. Diamond Head Hike. <b>Target Ranking:</b> 64th</p>	<p><b>Image:</b> </p> <p><b>Title:</b> Hawaiian 0033 <b>Topic:</b> #Hawaii travel #Hawaii Oahu Island Guide ... <b>Content:</b> It's off-season recently, so I finally don't have to queue. I like Honolulu, which is less crowded ... <b>Target Ranking:</b> 1st</p>
<p><b>Image:</b> </p> <p><b>Title:</b> pagani engine <b>Topic:</b> #64 Scale Car #Pagani #Engine #small scale car model <b>Content:</b> This should be the smallest Pagani engine. [laughing R]</p>	<p><b>Image:</b> </p> <p><b>Title:</b> LCD 1/64 Pagani Huayra r blue carbon <b>Topic:</b> #Alloy car model #Pagani #Pagani Huayra #model #1 to 64 car model # 64 scale car <b>Target Ranking:</b> 17th</p>	<p><b>Image:</b> </p> <p><b>Title:</b> 1/64 Once inside the car model, it's as deep as the sea. Released <b>Topic:</b> #64 Scale Car #Alloy car model #Car model ... <b>Target Ranking:</b> 17th</p>	<p><b>Image:</b> </p> <p><b>Title:</b> Front mid-mounted V12 White Horse <b>Topic:</b> #64 Scale Car #Alloy car model <b>Content:</b> I took a picture of the three white horses ... <b>Target Ranking:</b> 33rd</p>	<p><b>Image:</b> </p> <p><b>Title:</b> Enter the door. <b>Topic:</b> #64 scale car model #Alloy car model <b>Content:</b> Please give me some advice. <b>Target Ranking:</b> 16th</p>	<p><b>Image:</b> </p> <p><b>Title:</b> CM 1:64 Pagani zonda Revolution <b>Topic:</b> #Zonda #Pagani ZONDA # 64 scale car <b>Target Ranking:</b> 2nd</p>
<p><b>Image:</b> </p> <p><b>Title:</b> ☕️Share the learning content of the coffee training course without reservation <b>Topic:</b> #Coffee #Coffee Study... <b>Content:</b> ☕️Why cloth powder and pressing powder are important? ...</p>	<p><b>Image:</b> </p> <p><b>Title:</b> Espresso: Excess and Deficiency <b>Topic:</b> #coffee #Coffee Training #Italian espresso ... <b>Content:</b> ☕️When extracting espresso, a common situation encountered is the channel effect. ...</p>	<p><b>Image:</b> </p> <p><b>Title:</b> Coffee lovers who like Refreshing Latte can't miss it! <b>Topic:</b> #Coffee Bean Recommendation <b>Content:</b> HARU means "spring" and the bean lives up to its name. ☕️... <b>Target Ranking:</b> 52nd</p>	<p><b>Image:</b> </p> <p><b>Title:</b> Drinking coffee ☕️How to pour the concentrate? <b>Topic:</b> # Coffee Concentrate # Drink Coffee # Coffee Bean <b>Content:</b> I'm thinking buying some different pick-up concentrates... <b>Target Ranking:</b> 16th</p>	<p><b>Image:</b> </p> <p><b>Title:</b> Understanding Flannel... <b>Topic:</b> #flannel hand-brewed coffee #sociology in the café <b>Content:</b> It is best to use different flannel for different coffee beans... <b>Target Ranking:</b> 21st</p>	<p><b>Image:</b> </p> <p><b>Title:</b> Espresso: Excess and Deficiency <b>Topic:</b> #coffee #Coffee Training #Italian espresso ... <b>Content:</b> ☕️When extracting espresso, a common situation encountered is the ... <b>Target Ranking:</b> 1st</p>
<p><b>Image:</b> </p> <p><b>Title:</b> Ai painting picture sharing <b>Topic:</b> #Ai painting #painting #Looking for Painting Master</p>	<p><b>Image:</b> </p> <p><b>Title:</b> AI Painting Mooncake <b>Topic:</b> #AI painting Something #Notes Inspiration #AI painting #painting</p>	<p><b>Image:</b> </p> <p><b>Title:</b> Double happiness <b>Topic:</b> #romantic life recorder #AI painting #record life #AI painting has something... <b>Target Ranking:</b> 20th</p>	<p><b>Image:</b> </p> <p><b>Title:</b> None <b>Topic:</b> #Ai painting</p>	<p><b>Image:</b> </p> <p><b>Title:</b> My Lord, rest in peace   AIGC   Ai painting <b>Topic:</b> #Ai painting # Concept Design #AI #AiGC #Metaverse</p>	<p><b>Image:</b> </p> <p><b>Title:</b> Chang'e flies to the moon <b>Topic:</b> #Ai painting #art # Mid-Autumn Festival # Mid-Autumn Moon Appreciation #Chang'e <b>Target Ranking:</b> 2nd</p>

Figure 6: The visualization cases of some methods. Each line is a case, which the left two columns are the query note and target note, the other columns are the top-1 ranked notes for each method. We also show the target note ranking.